

Utah State University

DigitalCommons@USU

International Junior Researcher and Engineer
Workshop on Hydraulic Structures

6th International Junior Researcher and
Engineer Workshop on Hydraulic Structures
(IJREWS 2016)

May 30th, 11:45 AM - 12:00 PM

Prediction of Hydraulic Jump location in Some Types of Prismatic Channels using Numerical Modelling

M. A. Hafnaoui
University of Biskra

R. F. Carvalho
University of Coimbra

M. Debabeche
University of Biskra

Follow this and additional works at: <https://digitalcommons.usu.edu/ewhs>



Part of the [Civil and Environmental Engineering Commons](#)

Hafnaoui, M. A.; Carvalho, R. F.; and Debabeche, M., "Prediction of Hydraulic Jump location in Some Types of Prismatic Channels using Numerical Modelling" (2016). *International Junior Researcher and Engineer Workshop on Hydraulic Structures*. 1.

<https://digitalcommons.usu.edu/ewhs/2016/Session1/1>

This Event is brought to you for free and open access by the Conferences and Events at DigitalCommons@USU. It has been accepted for inclusion in International Junior Researcher and Engineer Workshop on Hydraulic Structures by an authorized administrator of DigitalCommons@USU. For more information, please contact digitalcommons@usu.edu.



Prediction of Hydraulic Jump location in Some Types of Prismatic Channels using Numerical Modelling

M. A. Hafnaoui^{1,2}, R. F. Carvalho³ and M. Debabeche¹

¹Research Laboratory of Civil Engineering, Hydraulics, Environment and Sustainable Development, - LARGHYDE -
University of Biskra
Biskra, Algeria

²Scientific and Technical Research Center on Arid Regions - CRSTRA -
Biskra, Algeria.

³Marine and Environmental Sciences Centre – MARE -
University of Coimbra
Coimbra, Portugal
E-mail: hafnaoui.amine@crstra.dz

ABSTRACT

The numerical modelling of free surface flows is important to understand their behaviour and predict undesired situations that may occur, as formation and location of hydraulic jump within irrigation channels. The Saint-Venant equations are most commonly used for practical modelling of this type of flows. There are many methods and numerical schemes used for the solution of these equations. The extension TVD plays an important role in minimizing the oscillations of the flow in the channels. In our work we used MATLAB® as a programming tool to develop a model based on 1D Saint-Venant equations and the MacCormack finite difference method with TVD extension scheme and after its validation we used it to calculate flow depth, velocity and predict the location of the hydraulic jump which is formed in prismatic sloped channels with different sections, such as rectangular and triangular sections.

Based on experimental trials at LARHYSS laboratory, University of Biskra, Algeria that allowed us to impose different upstream water depth and velocity (Froude number), downstream water depth as well as hydraulic jump locations, we were able to analyse the accuracy of the model to locate the hydraulic jump in triangular channels knowing the upstream and downstream depths. We present a matrix of flows ranging Froude numbers from 3 to 8, initial depth from 0.035 m to 0.05 m and velocities from 1.3 m/s to 4.5 m/s. Results of locations, as expected are better similar to experimental conditions for low slopes, the changing of slope and Froude number has an effect on its prediction uncertainty that can be estimated by a relation provided in this work.

Keywords: Saint-Venant equations, hydraulic jump, triangular channels, MacCormack scheme, free surface flows

1. INTRODUCTION

In irrigation systems several sills and gates are placed and measures of flow depth are fundamental to their management. Triangular channels allow the discharge prediction more accurately compared to rectangular channels, which are much more sensitive to water depth measurement.

A hydraulic jump is formed whenever flow changes from supercritical to subcritical flow. In this transition, water surface rises abruptly, surface rollers are formed, intense mixing occurs, air is entrained, and energy is dissipated (Gharangik and Chaudhry 1991). The dissipation capacity of a hydraulic jump evolving in a triangular channel is larger than that of a hydraulic jump evolving in a rectangular or trapezoidal channel, (Hager and Wanoschek 1987). Several researchers studied the hydraulic jump properties and location in recent years in horizontal rectangular channels (Hager and Bretz 1987; Hager 1992; Ead and Rajaratnam 2002; Carvalho et al. 2008; Chanson, 2009; Chanson and Carvalho 2015), in horizontal triangular channels (Hager and Wanoschek 1987; Achour and Debabeche 2003; and Debabeche and Achour 2007) and in a sloped triangular channel (Debabeche et al. 2009).

The hydraulic jump is formed at a location where the specific forces on both sides of the jump are equal. The hydraulic jump location and properties can be determined using continuity and momentum considerations. Chow (1959) computed the water surface profiles for supercritical flow in a channel, starting from the upstream end, and the subcritical flow starting from the downstream end. Mc-Corquodale and Khalifa (1983) used the strip-integral method to compute the jump length, water surface profile, and pressures at the bottom. To solve the Saint-Venant equation numerically, Abbott et al. (1969) used a finite-difference method and

Katopodes (1984) used the finite-element method (Gharangik and Chaudhry 1991). Garcia-Navarro et al. (1992) applied high-resolution MacCormack scheme TVD Saint-Venant equations to simulate unsteady flows in several applications. However the simulation of the hydraulic jump was always in low slopes or when there was a sudden decrease in the bottom slope.

The present study aims to analyse the location of a hydraulic jump predicted in a sloped triangular channel by the model based on 1D Saint-Venant equations for free surface flows. We used a high-resolution Mac Cormack scheme TVD to simulate hydraulic jumps location in channel up to slopes of 5 %. The work comprised more than 90 experimental hydraulic jumps in the laboratory which were reproduced with numerical simulations.

Every hydraulic jump in experimental conditions was formed on the apron by testing several different downstream water depths h_2 , setting specified sill height S , and adjust flow Q . (Figure 1a) shows the characteristics of hydraulic jump; h_1 is the upstream water depth measured at the toe of hydraulic jump, h_2 is the downstream water depth measured at the maximum surface level, α is the angle of inclination of the channel relative to the horizontal, L_j is the length of the hydraulic jump measured from the toe of the hydraulic jump to the section where maximum surface level occurs. The hydraulic jump is located at the upstream of the channel for the channel downstream depth h is less than h_2 , the hydraulic jump moves downstream (Figure 1b). However, the jump is pushed back as shown in (Figure 1c) if the channel downstream depth is higher than h_2 (Chaudhry 2008). In experimental conditions position can be settled by adjusting flow.

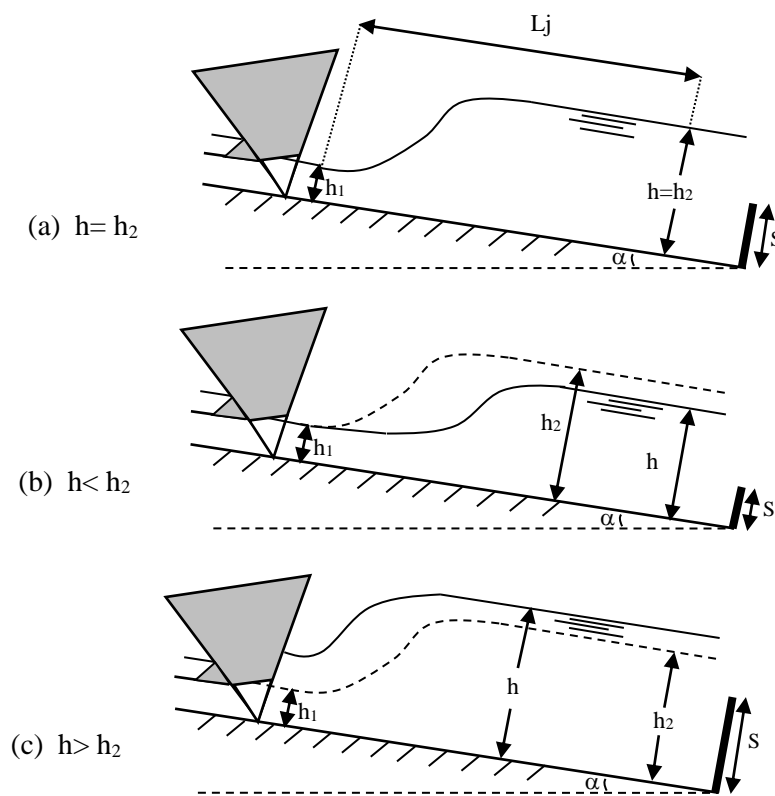


Figure 1. Location of hydraulic jump scheme

Next section presents the description of the experimental tests in the laboratory, the governing equations and numerical scheme used to simulate the hydraulic jumps. Section 3 presents and discusses the results of the numerical simulations in rectangular and triangular channels for different slopes as it was founded that numerical simulation doesn't predict accurately the hydraulic jump location for all hydraulic jump tests. The main conclusions are presented in Section 4.

2. METHODOLOGY

2.1. Description of the experimental model and tests

The experiments of hydraulic jump were made at the Research Laboratory in Subterranean and Surface Hydraulics (LARHYSS) of the Hydraulic Department of University of Biskra. The rectangular channel was 7 m long and 0.295 m wide (Debabeche 2003) and the triangular channel was symmetrical with 3 m long and a triangular cross section with the bottom angle of 90° . A circular pipe of 0.115 m diameter connected the channel with pressure box, on which was inserted a pressure convergent of triangular cross section opening directly into the channel. The role of the pressure convergent was to generate the flow at high velocity as shown in Figure 2. The Figure 3 shows a general view of the triangular channel and in Figure 4 an aspect of the hydraulic jump in the sloped triangular channel for ($F_1 = 6.32$; $s = 0.22$ m ; $L_j = 1.22$ m ; $h_2 = 0.1882$ m, $\text{tang}(\alpha) = 0.05$).

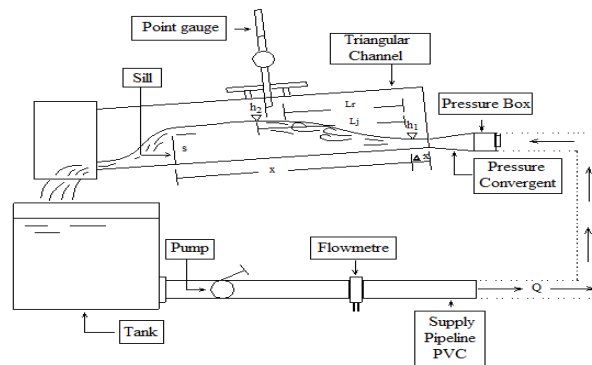


Figure 2. Experimental model



Figure 3. General view of the experimental channel



Figure 4. Hydraulic jump in a sloped triangular channel

The experimental study was conducted in three initial upstream water depth $h_1 = 0.035$, 0.04 and 0.05 m. For each chosen upstream water depth, h_1 , there were six different slopes tested characterized by $\text{tang}(\alpha) = 0\%$, 1% , 2% , 3% , 4% and 5% . A large range of Froude number F_1 from 3 to 8 was tested.

The flow was measured by a rectangular weir, connected with the triangular channel with its downstream part described by the following equation: $Q = 0.3794B(2g)^{0.5} \beta(1+0.16496\beta^{2.0716})^{1.5}h^{1.5}$, obtained by Hachemi (2006) where B is the width of the channel and β is the form ratio coefficient. The water depth in the channel was measured by a level indicator (limnimeter). The water level measurement range can be set to ± 0.01 m. The Froude number is calculated from the following universal relation: $F_1^2 = 2Q^2(gm^2h_1^5)^{-1}$ valid for a symmetrical triangular channel, where m is the cotangent of the angle of inclination of the channel.

2.2. Governing Equations and Numerical Scheme

The Saint-Venant equations (1871) represented by the mass and the momentum conservation equations are used for modeling non-stationary flows in gradually and rapidly varied flow at free surface, (Maher 2009). The Saint-Venant equations for one-dimensional flow can be written as follows:

$$\frac{\partial A}{\partial t} + \frac{\partial Q}{\partial x} = 0 \quad (1)$$

$$\frac{\partial Q}{\partial t} + \frac{\partial}{\partial x} \left(\frac{Q^2}{A} + gI_1 \right) = -gAs - gAJ + gI_2 \quad (2)$$

where x is the distance along the channel bed, t is the time, A is the flow area, Q is the flow in the x -direction, I_1 is the pressure force, I_2 is the pressure forces due to longitudinal width variations, g is the gravitational acceleration, s is the channel bed slope and J is the friction slope. They are valid for horizontal and low slope, as the pressure distribution is considered hydrostatic, the fluid is incompressible, and the velocity is assumed constant in the section.

The friction slope can be expressed using the Manning's equation as:

$$J = \frac{|Q|Q}{K_s^2 A^2 R^{4/3}} \quad (3)$$

where K_s is the Strickler's roughness coefficient; and R is the hydraulic radius. The MacCormack scheme is an explicit finite difference method which belongs to the class of methods called fractional step method. It resulted from changes in the methods of two steps based on the expansion of second order Taylor series, specifically in the method of Lax Wendroff, this scheme guarantees the approximation in second order in space and time (Carmo 2009). For the application of the MacCormack scheme, the Saint-Venant equations could be written as:

$$\frac{\partial U}{\partial t} + \frac{\partial F}{\partial x} = S \quad (4)$$

with

$$U = \left\{ \begin{matrix} \bar{A} \\ Q \end{matrix} \right\} \quad F = \left\{ \begin{matrix} Q \\ \frac{Q^2}{A} + gI_1 \end{matrix} \right\} \quad S = \left\{ \begin{matrix} 0 \\ -gAs - gAJ + gI_2 \end{matrix} \right\} \quad (5)$$

The MacCormack scheme is explicit and applied with two-step: initially a calculation based on the values of variables in the previous time (predictor) and then a correction step based on the predicted values (corrector). The accuracy of the second order is guaranteed by the discretization in two symmetrical steps.

Predictor:

$$U_i^{(1)} = U_i^n - \frac{\Delta t}{\Delta x} [F_{i+1}^n - F_i^n] + \Delta t S_i^n \quad (6)$$

Corrector:

$$U_i^{n+1} = \frac{1}{2} \left[U_i^n + U_i^{(1)} - \frac{\Delta t}{\Delta x} (F_i^{(1)} - F_{i-1}^{(1)}) + \Delta t S_i^{(1)} \right] \quad (7)$$

For the stability of The MacCormack scheme, as of other explicit methods, it is necessary to check the Courant-Friedrichs-Lewy (CFL) condition:

$$\Delta t = C_n \frac{\Delta x}{\max(|U| + \sqrt{gy})} \quad (8)$$

where C_n is Courant number and y is hydraulic depth. The resolution of Saint-Venant equations using MacCormack scheme can generate numerical oscillations. To reduce these oscillations, an extension of high-resolution based on the theory of the Total Variation Diminishing TVD could be introduced into the MacCormack method, which leads to a more robust model. The TVD extension on the MacCormack method can be written as:

$$U_i^{n+1} = U_i^{(2)} + \left(\tilde{R}_{i+\frac{1}{2}} \tilde{D}_{i+\frac{1}{2}} - \tilde{R}_{i-\frac{1}{2}} \tilde{D}_{i-\frac{1}{2}} \right) \quad (9)$$

where \tilde{R} is the right-eigenvector matrix corresponding to the approximated Jacobian, and \tilde{D} is a scheme dependent vector function. Details could be founded in (Garcia-Navarro et al. 1992) work who studied the role of TVD-MacCormack scheme for the reduction of oscillations resulting from the classical method of

MacCormack. This study was done in rectangular and trapezoidal channels with slope and the presence of hydraulic jump, after a comparison between a classical scheme of MacCormack and extension TVD, the results showed an effectiveness to minimize the oscillations by TVD- MacCormack scheme.

2.3. Model validation and application to study hydraulic jump characteristics

MATLAB® Model was developed based on 1D Saint-Venant equations and the MacCormack finite difference scheme with TVD extension described above, was validated with literature data “benchmarkdata” (Mendes, 2001) and was used to simulate a large range of hydraulic jumps tested in the laboratory. Figure 5 shows the numerical results of the flow $Q = 0.18 \text{ m}^3/\text{s}$ in a rectangular channel of 25 m length with water depth $h_1 = 0.33 \text{ m}$ over an obstacle which induce a subcritical-supercritical-subcritical regime ($t = 100 \text{ s}$ and $\Delta x = 0.1 \text{ m}$). The comparison of the analytical and numerical solutions shows that the results are similar. It is noticed an insignificant difference in the change of the super to sub-critical regime.

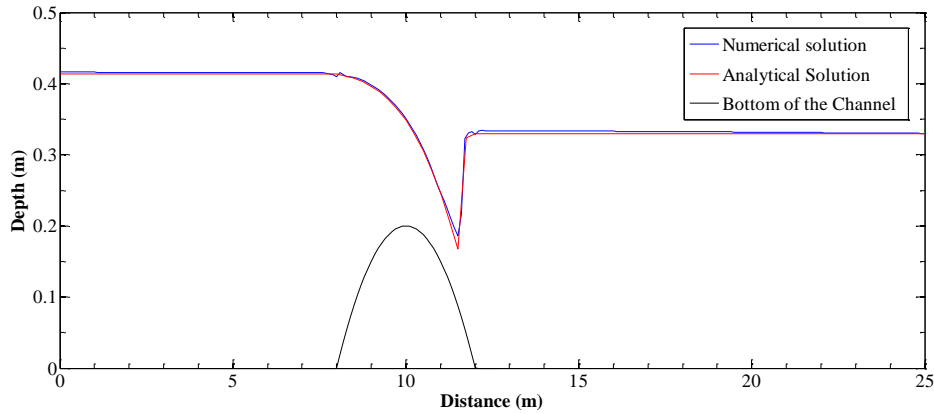


Figure 5. Numerical simulation of flow over an obstacle

The selected tested simulations are presented in Table 1 for the rectangular channel and in Table 2 for the triangular channel. Tables 1 and 2 shows the main characteristics of the hydraulic jumps accordingly the experimental tests and the results of hydraulic jump location simulated with the presented model. The model allowed quantifying uncertainty of the simulation results reproducing hydraulic jumps. Courant number used in the simulations varied from 0.2 ($F_1 > 7$) and 0.5 ($F_1 = 3$).

Table 1: Hydraulic jump in rectangular channel simulations

<i>Slope: $s = 0.00$; mesh: $dx = 0.1 \text{ m}$; time test: $t = 60 \text{ s}$; Coefficient of roughness: $K_s = 100 \text{ m}^{1/3}\text{s}^{-1}$</i>							
<i>results from experimental tests</i>						<i>results from numerical model</i>	
<i>Experiment number</i>	<i>Flow Q (m^3/s)</i>	<i>Froude number F_1</i>	<i>upstream water depth h_1 (m)</i>	<i>downstream water depth h_2 (m)</i>	<i>sequentdepths ratio $Y = h_2/h_1$</i>	<i>Location of h.jump L_c (m)</i>	<i>Lc/L</i>
1	0.02527	3.42	0.040	0.1859	4.65	0.1	0.014
2	0.02737	5.70	0.030	0.2390	7.97	0.1	0.014
3	0.01869	7.15	0.020	0.1914	9.57	0.1	0.014

Table 2: Hydraulic jump in triangular channel simulations

<i>mesh : $dx = 0.1 \text{ m}$; time test : $t = 60 \text{ s}$; Coefficient of roughness: $K_s = 100 \text{ m}^{1/3}\text{s}^{-1}$</i>								
<i>results from experimental tests</i>							<i>results from numerical model</i>	
<i>Experiment number</i>	<i>Slope s</i>	<i>Flow Q (m^3/s)</i>	<i>Froude number F_1</i>	<i>upstream water depth h_1 (m)</i>	<i>downstream water depth h_2 (m)</i>	<i>sequentdepth s ratio $Y = h_2/h_1$</i>	<i>Location of h. jump L_c (m)</i>	<i>Lc/L</i>
1	0.00	0.00278	3.92	0.040	0.1038	2.60	0.6	0.2069
2	0.00	0.00227	4.48	0.035	0.1013	2.89	0.3	0.1034
3	0.00	0.00327	6.44	0.035	0.1339	3.83	0.1	0.0345
4	0.00	0.00868	7.01	0.050	0.2013	4.03	0.1	0.0345
5	0.00	0.00991	8.00	0.050	0.2213	4.43	0.1	0.0345

6	0.02	0.00342	2.76	0.05	0.1537	3.07	0.3	0.1034
7	0.02	0.00457	3.69	0.05	0.1730	3.46	0.3	0.1034
8	0.02	0.00311	4.39	0.04	0.1502	3.76	0.7	0.2414
9	0.02	0.00390	5.50	0.04	0.1670	4.18	0.8	0.2759
10	0.02	0.00281	5.53	0.035	0.1403	4.01	1.1	0.3793
11	0.02	0.00378	7.45	0.035	0.1722	4.92	0.8	0.2759
12	0.05	0.00373	3.01	0.05	0.1451	2.90	2.1	0.7241
13	0.05	0.00469	3.78	0.05	0.1681	3.36	1.8	0.6207
14	0.05	0.00292	4.12	0.04	0.1458	3.65	1.9	0.6552
15	0.05	0.00581	4.69	0.05	0.2001	4.00	1.5	0.5172
16	0.05	0.00726	5.87	0.05	0.2404	4.81	1.3	0.4483
17	0.05	0.00424	5.98	0.04	0.1764	4.41	1.7	0.5862
18	0.05	0.00337	6.65	0.035	0.1757	5.02	1.5	0.5172
19	0.05	0.00581	8.20	0.04	0.2215	5.54	1.4	0.4828
20	0.05	0.00433	8.52	0.035	0.2042	5.83	1.4	0.4828

3. RESULTS AND DISCUSSION

3.1. Location of hydraulic jump predicted through numerical simulations

In this part the numerical simulation in rectangular and triangular horizontal channels is presented, and the location of the hydraulic jump in a triangular channel with different slopes is analyzed. Figures 6 and 7 illustrate the hydraulic jump profile obtained by the simulations of horizontal rectangular and triangular channels, respectively.

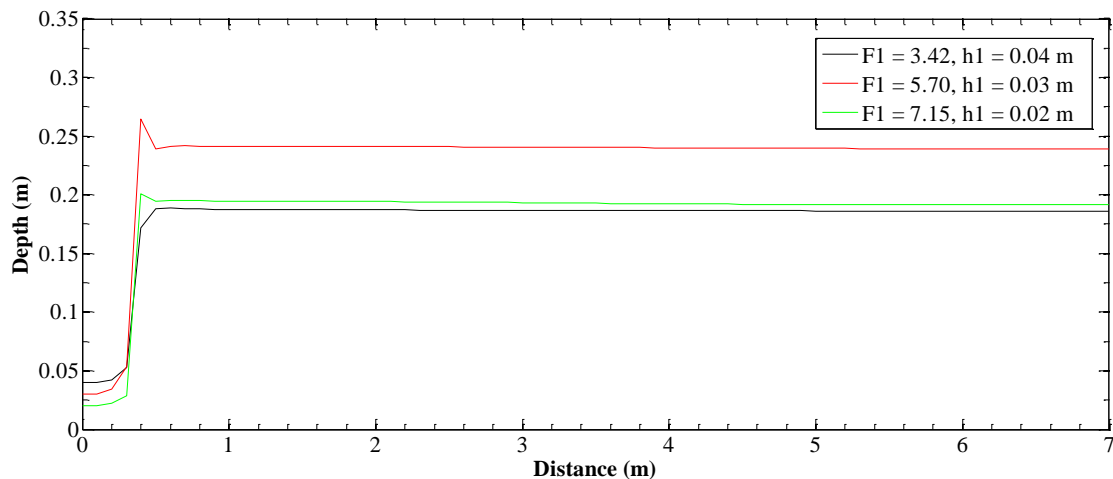


Figure 6. Hydraulic jump profile in a rectangular section channel predicted by numerical simulations ($s = 0$)

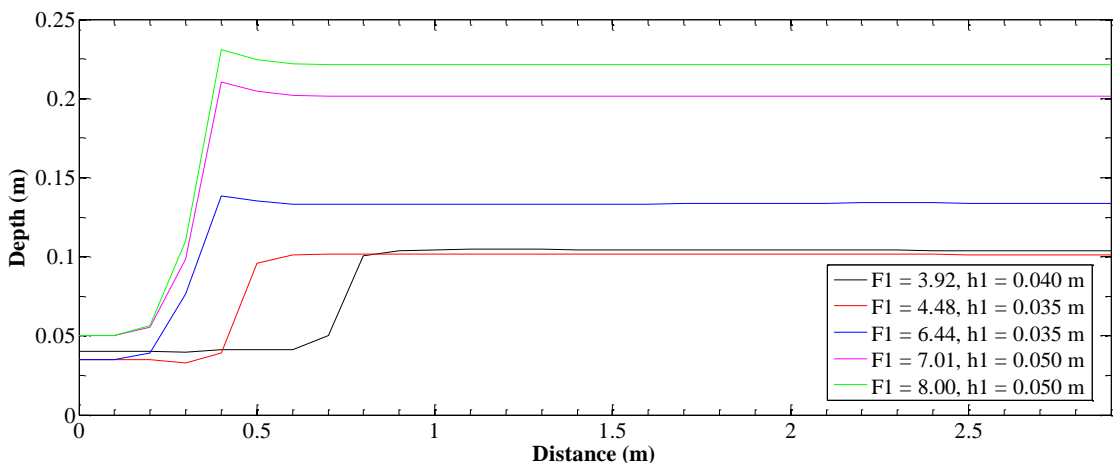


Figure 7. Hydraulic jump profile in a triangular section channel predicted by numerical simulations ($s = 0$)

Analysing these results, we can remark the following:

- For the rectangular section the location of hydraulic jump is placed upstream as was observed in experimental tests.
- For the triangular section and for high Froude number the location of the hydraulic jump is placed in upstream of channel; however for low Froude numbers, at the simulation 1 ($F_1 = 3.92, h_1 = 0.04$) and 2 ($F_1 = 4.48, h_1 = 0.035$), the location of hydraulic jump is previewed slightly downstream.

The prediction of the location of the hydraulic jump in a triangular channel with variable slope using Saint-Venant equation are illustrated in Figures 8 and 9. In our numerical simulations we chose the slope 0.02 and 0.05. As initial conditions it was used the flow Q and the upstream water depth h_1 , and we imposed the boundary condition downstream water depth equal to h_2 . It was fixed two first points in the upstream and two last points in the downstream of the channel to give the model more rigidity, the time test $t = 60$ s and $\Delta x = 0.1$ m.

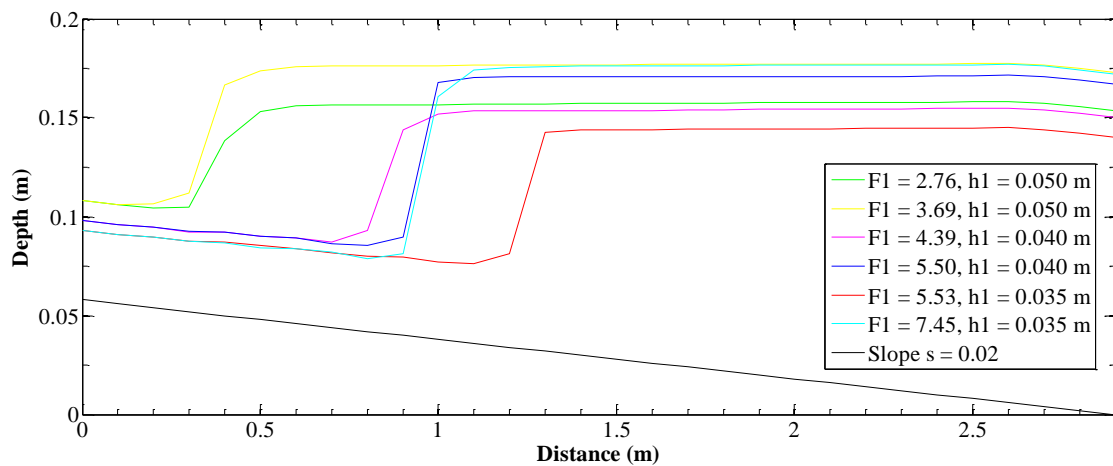


Figure 8. Hydraulic jump profile in triangular section channel predicted by numerical simulation ($s = 0.02$)

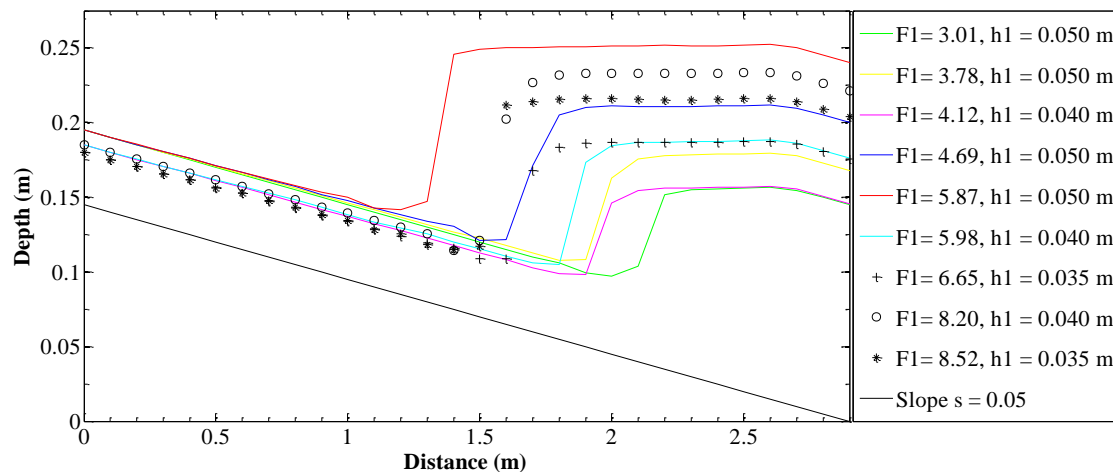


Figure 9. Hydraulic jump profile in triangular section channel predicted by numerical simulation ($s = 0.05$)

It is noticed that the hydraulic jump takes different locations in the channel. In the horizontal slope most the locations of the hydraulic jump are in the upstream of the channel as settled in experimental conditions, as well as, for hydraulic jump with small Froude numbers with slope equal to 0.02. However for larger Froude numbers the hydraulic jump moves downstream. Whenever the slope increases the hydraulic jump moves more downstream. This can be returned to the validity of the Saint-Venant equations for low slopes and also to the measurement of the downstream water depth h_2 .

It was observed in the experimental tests, for larger slopes and large Froude numbers, that was difficult to measure the downstream water depth h_2 accurately, because the free surface flow is not constant and may increase slightly to downstream given underestimate downstream water depth, h_2 (h_2 measurements are ± 0.01 m accurately). We then increased downstream water depth h_2 to settle the hydraulic jump in the upstream of the channel, as verified in experimental conditions, and we studied the relation between the numerical simulation

imposed downstream water depth h_2 (h_2 simulated) which gives the hydraulic jump location in channel upstream extremity and other characteristics of the hydraulic jump.

3.2. Relation between h_2 and the location of hydraulic jump

Figure 10 shows the variation of the sequent depths ratio simulated and experimental depending to Froude number F_1 for slopes 0.02 and 0.05. Relations between the sequent depths ratio Y_{sim} and Y_{exp} with Froude number F_1 and slope s were founded. The relations obtained are shown in the Figure 11 are following: Eq. (10) variation of the sequent depths ratio Y_{sim} depending on Froude number F_1 and slope, Eq. (11) variation of the sequent depths ratio Y_{exp} depending on Froude number F_1 and slope.

$$\frac{h_{2\ sim}}{h_1} = a + bF_1 + cF_1^2 + \frac{d}{tg\alpha} \quad (10)$$

where $a = 3.3622$, $b = 0.9703$, $c = -0.0582$ and $d = -0.0432$; with $r^2 = 0.97$

$$\frac{h_{2\ exp}}{h_1} = a + bF_1 + cF_1^2 + \frac{d}{tg\alpha} \quad (11)$$

where $a = 1.5254$, $b = 0.5869$, $c = -0.0078$ and $d = -0.0083$; with $r^2 = 0.93$

These relations could give the difference between downstream water depth, the h_{2exp} (observed in the laboratory) and h_{2sim} (that lead to a hydraulic jump simulation located at upstream of the channel) in function on Froude and slope.

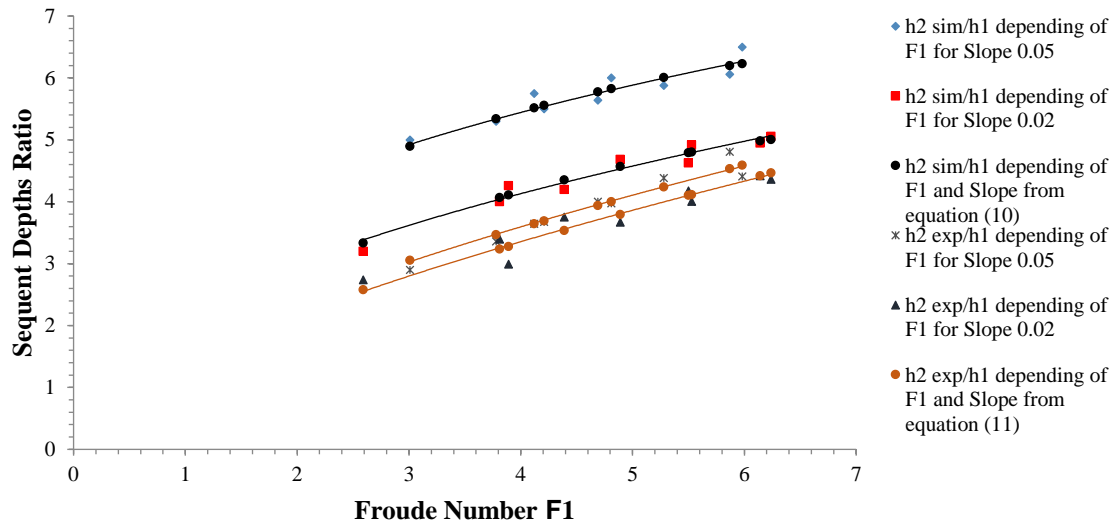


Figure 10. Variation of the sequent depths ratio simulated/experimental depending to Froude number and slope

Subtracting the equations (10) and (11), we reach to relation (12).

$$\frac{h_s}{h_1} = a + bF_1 + cF_1^2 + \frac{d}{tg\alpha} \quad (12)$$

where $a = 1.8368$, $b = 0.3834$, $c = -0.0504$ and $d = -0.0349$; with $r^2 = 0.93$

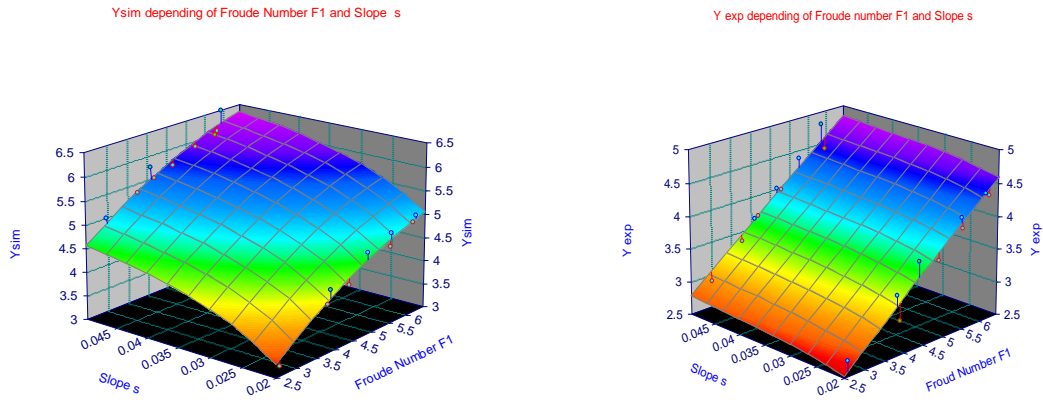


Figure 11. Relation between conjugate depths, Froude number and slope from the equations (10) and (11)

Through this last relation we can calculate the downstream water depth required to include in the downstream boundary condition in the simulation model for the hydraulic jump be located on upstream of the channel as verified in experimental conditions.

3.3. Location of hydraulic jump

In this part we study the relation between the location of the hydraulic jump and the difference between water depth $h_s = h_{2sim} - h_{2exp}$, Figure 12 represents relations between Lc/h_1 , h_s/h_1 and slope s .

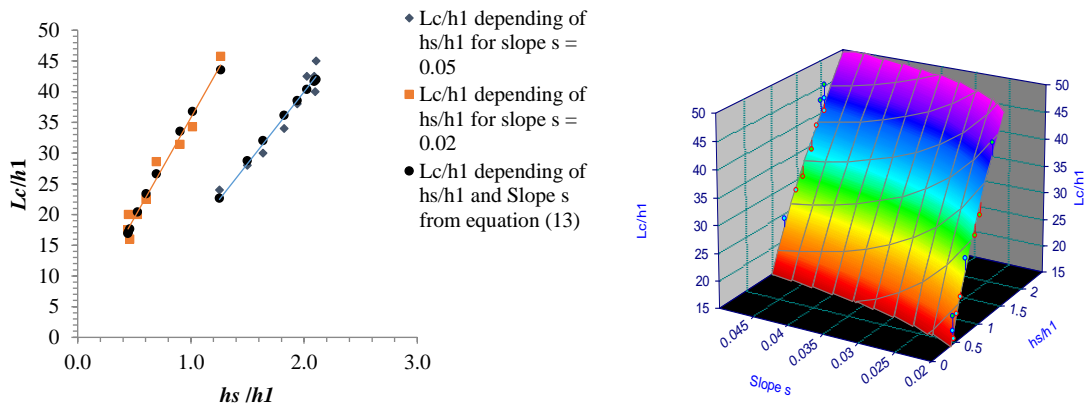


Figure 12. Relation between Lc/h_1 and h_s/h_1 : (left) Lc/h_1 and h_s/h_1 and (right) Lc/h_1 , h_s/h_1 and slope s

The results showed a linear relation between Lc/h_1 and h_s/h_1 for both slopes 0.02 and 0.05. The general equation obtained for the variation of Lc/h_1 depending with h_s/h_1 and slope s is:

$$\frac{Lc}{h_1} = a + b \frac{h_s}{h_1} + \frac{c}{(tg\alpha)^{1.5}} \quad (13)$$

where $a = -49.55$, $b = 58.28$ and $c = 0.08$; with $r^2 = 0.96$

4. CONCLUSION

In this work a MATLAB® model based on Saint-Venant equations and the TVD MacCormack explicit scheme for different sections was developed. It was applied to simulate a large range of hydraulic jumps tested in the laboratory with rectangular and triangular channels for Froude numbers ranging from 3 to 8. The location of a hydraulic jump was studied in a sloped triangular channel previewed by the model as some differences in the hydraulic jump location prediction compared with experimental tests were found. These differences with hydraulic jump characteristics which allows to quantify uncertainty in measured h_2 to reproduce hydraulic jumps location were related.

For using model based on Saint Venant equations to simulate flows on sloped triangular channels, care should be taken if a hydraulic jump forms in the channel as their location could be predicted slightly downstream if downstream water depth are not measured in a required distance from the jump. It is recommend to use (12) to predict location more accurately or using also (13) to know the uncertainty of L_c .

5. ACKNOWLEDGMENTS

The first author would like to acknowledge the support of mesrs (Ministry of Higher Education and Scientific Research, Algeria) through the scholarship PNE.

Second author would also like to acknowledge for the support of FCT (Portuguese Foundation for Science and Technology) through the Project UID/MAR/04292/2013 financed by MEC (Portuguese Ministry of Education and Science) and FSE (European Social Fund), under the program POCH (Human Capital Operational Programme).

6. REFERENCES

- Abbott, M. B., Marshall, G., and Rodenhuis, G. S. (1969). Amplitude-Dissipative and Phase-Dissipative Scheme for Hydraulic Jump Simulation, *Proc., 13th Congress*, Inter. Assoc. Hyd. Research, Tokyo, pp.313-329.
- Achour, B. (1989). Jump flow meter in a channel of triangular cross-section without weir: *Journal of Hydraulic Research.*, 27(2), 205-214.
- Achour, B., and Debabeche, M. (2003). Control of hydraulic jump by sill in a triangular channel: *Journal of Hydraulic Research*, 41(3), 97-103.
- Carmo, J.S. (2009). *Modelação em Hidráulica Fluvial e Ambiente*, imprensa da universidade de Coimbra.
- Carvalho, R.F., Lemos, C.M., and Ramos, C.M. (2008). Numerical computation of the flow in hydraulic jump stilling basins: *Journal of Hydraulic Research.*, 46(6), 739–752.
- Chanson, H., (2009) Current knowledge in hydraulic jumps and related phenomena. A survey of experimental results, *European Journal of Mechanics B/Fluids* 28.
- Chanson, H., and Carvalho, R. F. (2015). Chapter 4, Hydraulic Jumps, in *Energy Dissipation in Hydraulic Structures*, IAHR Monograph, *CRC Press*, Taylor & Francis Group, Leiden, The Netherlands, 168 pages.
- Chaudhry, M. H. (2008). *Open-Channel Flow*, University of South Carolina, Columbia, *Springer Science and Business Media, LLC*.
- Chow, V. T., (1959), *Open Channel Hydraulics*, *McGraw-Hill Book Company*.
- Debabeche, M., (2003). Le ressaut hydraulique dans les canaux prismatiques, université de Biskra, Algérie.
- Debabeche, M., and Achour, B. (2007). Effect of sill in the hydraulic jump in a triangular channel: *Journal of Hydraulic Research.*, 45(1), 135–139.
- Debabeche, M., Cherhabil, S., Hafnaoui, A., and Achour, B. (2009). Hydraulic Jump in a Sloped Triangular Channel: *Canadian Journal of Civil Engineering.*, 36, 655-658.
- Ead, S.A., and Rajaratnam, N. (2002). Hydraulic jump on corrugated beds: *Journal of Hydraulic Engineering.*, 128(7), 656-663.
- Gharangik, A. and Chaudhry, M. (1991). Numerical Simulation of Hydraulic Jump: *Journal of Hydraulic Engineering*, 9(1195), 1195-1211.
- García-Navarro, P., Alcrudo, F., and Saviron, J. M. (1992). 1-D Open-Channel Flow Simulation Using TVD-McCormack Scheme: *Journal of Hydraulic Engineering.*, 118, 1359-1372.

- Hachemi, R.L. (2006). Analyse d'un écoulement au travers d'un contraction latérale, université de Biskra.Algérie.
- Hager,W. H. (1992). Energy dissipators and hydraulic jump. *Kluwer Academic Publishers*, Dordrecht, The Netherlands. 288 pages.
- Hager, W. H., and Bretz, N. V. (1987). Hydraulic jumps at positive and negative steps: *Journal of Hydraulic Research*.,24(4), 237-253.
- Hager, W. H., and Wanoschek, R. (1987). Hydraulic jump in triangular channel: *Journal of Hydraulic Research*., 25(5), 549-564.
- Hubert, C. (2009). Current knowledge in hydraulic jumps and related phenomena.A survey of experimental results: *European Journal of Mechanics B/Fluids*., 28 (2009), 191-210.
- Katopodes, N. D. (1984). A Dissipative Galerkin Scheme for Open-Channel Flow: *Journal of Hydraulic Engineering*, 110(4), 450-466.
- Maher, A. (2005). Sur les méthodes de discrétisation numérique de problèmes hyperboliques non linéaires appliquées aux équations de Barré de Saint-Venant pour la modélisation de l'hydraulique en réseau d'assainissement, Université Louis Pasteur de Strasbourg, École Nationale du Génie de l'Eau et de l'Environnement de Strasbourg.
- McCorquodale, J. A. and Khalifa, A. (1983). Internal Flow in Hydraulic Jumps: *Journal of Hydraulic Engineering*, 109(5), 684-701.
- Mendes, P.J. (2001). Contribuição para o Estudo da Modelação das Ondas de Cheia Provocadas pela Ruptura de Barragens, Universidade de Coimbra.